Pharmacoinformatics-based identification of anti-bacterial Catalase-peroxidase enzyme inhibitors

Chaitanya Sadashiv Jangam[#1], Shovonlal Bhowmick[#2], Rekha Dhondiram Chorge[1], Lomate Dhanraj Bharatrao[1], Pritee Chunarkar Patil[1], Rupesh V. Chikhale[3], Nora Abdullah AlFaris[4], Jozaa zaidan ALTamimi[4], Saikh Mohammad Wabaidur[5], Md Ataul Islam[*6,7,8]

[1]*Department of Bioinformatics, Rajiv Gandhi Institute of IT and Biotechnology, Bharati Vidyapeeth Deemed University, Pune-Satara Road, Pune, India.*
[2]*Department of Chemical Technology, University of Calcutta, 92 A.P.C. Road, Kolkata, India.*
[3]*Faculty of Pharmacy, The Maharaja Sayajirao University of Baroda, Vadodara, Gujarat 390 001, India.*
[4]*Nutrition and Food Science, Department of Physical Sport Science, Princess Nourah bint Abdulrahman University, P.O. Box 84428, Riyadh 11671, Saudi Arabia.*
[5]*Department of Chemistry P.O. Box 2455, College of Science, King Saud University, Riyadh, 11451, Saudi Arabia.*
[6]*Division of Pharmacy and Optometry, School of Health Sciences, Faculty of Biology, Medicine and Health, University of Manchester, Oxford Road, Manchester M13 9PL, United Kingdom.*
[7]*School of Health Sciences, University of Kwazulu-Natal, Westville Campus, Durban, South Africa.*
[8]*Department of Chemical Pathology, Faculty of Health Sciences, University of Pretoria and National Health Laboratory Service Tshwane Academic Division, Pretoria, South Africa.*

[#]Contributed equally and both can be considered as the first author.

Correspondence should be addressed to Md Ataul Islam, Division of Pharmacy and Optometry, School of Health Sciences, Faculty of Biology,Medicine and Health, University of Manchester, Oxford Road, Manchester M13 9PL, United Kingdom.
Email: ataul.islam80@gmail.com

Highlights

- Wild type Catalase-peroxidase enzyme (WT katG) mutated into five mutant katG (MT katG).
- Molecular docking was performed WT and MT katG.
- Screening was performed based on binding energy of Isoniazid and promising katG inhibitors proposed.
- MD simulation was performed for MT katG-proposed molecules complex.
- Binding energy of proposed molecules was calculated using MM-PBSA approach.

Graphical abstract

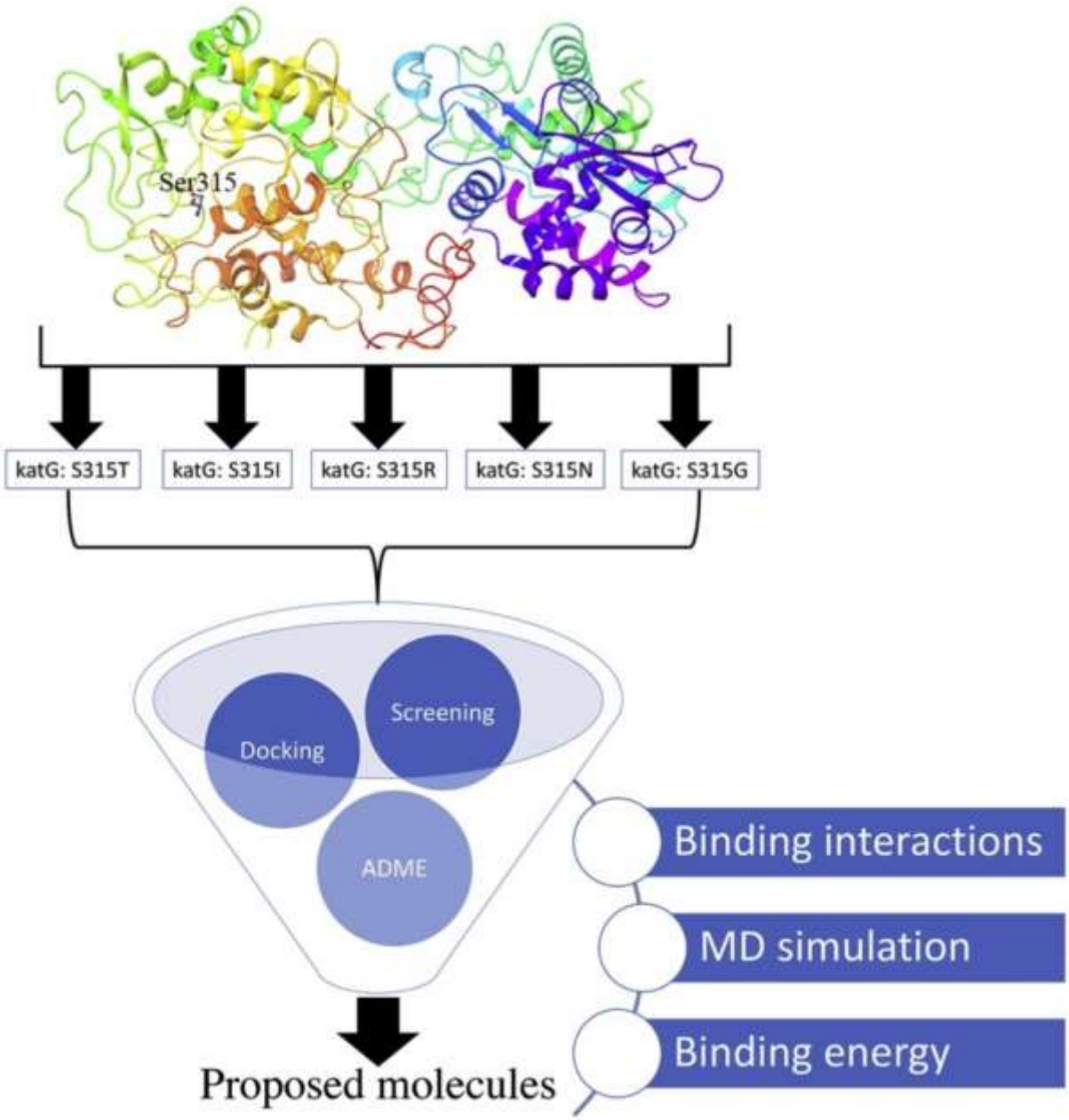

Abstract

Tuberculosis (TB) is an infectious disease caused by *Mycobacterium tuberculosis* (Mtb). In the present age, due to the rapid increase in antibiotic resistance worldwide, TB has become a major threat to human life. Regardless of significant efforts have been inclined to improve the healthcare systems for improving diagnosis, treatment, and anticipatory measures controlling TB is challenging. To date, there are no such therapeutic chemical agents available to fight or control the bacterial drug-resistance. The catalase-peroxidase enzyme (katG) which encoded by the *katG* gene of Mtb is most frequently getting mutated and hence promotes Isoniazid resistance by diminishing the normal activity of katG enzyme. In the current study, an effort has been intended to find novel and therapeutically active antibacterial chemical compounds through pharmacoinformatics methodologies. Initially, the five mutant katG were generated by mutation of Ser315 by Thr, Ile, Arg, Asn, and Gly followed by optimization. About eight thousand small molecules were collected from the Asinex antibacterial library. All molecules were docked to five mutant katG and wild type katG. To narrow down the chemical space several criteria were imposed including, screening for highest binding affinity towards katG proteins, compounds satisfying various criterion drug-likeliness properties like Lipinski's rule of five (RO5), Veber's rule, absorption, distribution, metabolism, and excretion (ADME) profile, and synthetic accessibility. Finally, five molecules were found to be important antibacterial katG inhibitors. All the analyzed parameters suggested that selected molecules are promising in nature. Binding interactions analysis revealed that proposed molecules are efficient enough to form a number of strong binding interactions with katG proteins. Dynamic behavior of the proposed molecules with katG protein was evaluated through 100ns of MD simulation. Parameters calculated from the MD simulation trajectories adjudged that all molecules can form stable complexes with katG. High binding free energy of all proposed molecules definitely suggested strong affection towards the katG. Hence, it can be concluded that proposed molecules might be used as antibacterial chemical component subjected to experimental validation.

Keywords: Catalase-peroxidase enzyme; Pharmacoinformatics; Virtual screening; Molecular docking; Molecular dynamics, Binding energy

1. Introduction

Among many severe infectious and communicable diseases, tuberculosis (TB) is regarded as the most serious and challenging global public health problems, majorly induced by the bacterium,

Mycobacterium tuberculosis (Mtb) – a bacillus agent [1, 2]. The burden of TB infections remains strong-growing realities despite the implementation of cost-effective vaccination strategy for infants with Bacille Calmette-Guerin (BCG), as its outcome is not remarkable or fully effective to control the Mtb infection. According to the Global Tuberculosis Report 2018, published by the World Health Organization (WHO), approximately 1.3 million deaths occur in 2017 worldwide, due to TB infection [3]. Moreover, it is also reported that countries like China, Ethiopia, India, Indonesia, Kenya, Mozambique, etc. are among the top list of 30 high TB burden countries. The severity of this disease burden accounted for the number of incident cases per 10,0000 population per year with not only TB infection alone, but also with TB/human immune deficiency virus (TB/HIV) co-infection and multidrug resistance TB (MDR-TB) infection in these countries [3]. Treatment of MDR-TB infection extremely difficult as because of Mtb get resistance to at least two first-line anti-tubercular drugs - Rifampicin (**RIF**) and Isoniazid (**INH**) [2, 4, 5]. Resistance to such particular drugs typically occurs due to chromosomal replication errors or gene mutations in Mtb which encode specific drug targets [6]. Usually, any drug resistant Mtb strains are highly pathogenic in nature and show great potential for dissemination [7]. Moreover, treatment of MDR-TB requires much longer than treatment of drug-susceptible TB. However, to treat MDR-TB, currently available first-line anti-tuberculous drugs (rifampicin, isoniazid, ethambutol, pyrazinamide, and streptomycin) are more toxic and have critical adverse effects [5], and most importantly, majority of those drugs are developed long back almost more than 40 years [4]. Although, availability of such effective frontline chemotherapeutic regimen against Mtb, still morbidity and mortality rates of TB remains very high. Therefore, factors associated with TB controls and treatments regimens are needed to be fully supervised over the obstacle facing today. Recently employed genome-wide association study of MDR and extensively drug-resistant clinical Mtb isolates from more than 30 countries have identified resistance causing different mutations and resistant phenotypes that may give understanding on the molecular mechanism of drug resistance which profoundly will assist in designing of next-generation novel antibiotics [8].

The Mtb cell wall is unique due to the presence of mycolic acid and since the last few decades, the focus has been shifted on targeting the synthetic components of the cell wall. One of the main enzymes in the synthetic process is catalase-peroxidase enzyme (katG). It is well-testified fact that katG - heme enzyme which encoded by the *katG* gene of Mtb is most frequently getting mutated and hence promotes **INH** resistance by diminishing the normal activity of katG enzyme [8]. Normally, the prodrug **INH** activated by this enzyme and the activated form inhibits mycolic acid biosynthesis by

means of preventing cell wall synthesis in Mtb [5]. However, mutations in *katG* led inability to activate **INH**. Mutation of katG at Ser315 is most prevalent and virulent among other several mutations have been identified so far [5, 9-12]. In our previous studies, we have designed and identified some potential anti-bacterial and anti-tubercular chemical entities as DNA gyrase B (Gyr B) inhibitors using *de novo* design technique, pharmacophore-based virtual screening, molecular docking and dynamics simulations studies [4, 13]. In the present study, we employed advanced multi-pharmacoinformatics techniques to closely looked into the most prevalent five types of mutations observed in katG *viz.* S315T, S315I, S315R, S315N, and S315G to identify novel anti-tubercular drugs [14]. Additionally, the structure-based drug design (SBDD) strategy for developing novel molecular entities for **INH** resistance specific different variant katG proteins are compared with wild type Mtb - katG protein. Earlier, numbers of studies have adopted computational molecular modeling techniques for accelerating the anti-tubercular drug developmental process applied to various multifunctional biological target receptors or proteins of Mtb [15-25]. However, very few studies were employed earlier targeting specifically selected five mutation types (at codon S315 of katG) for enhancing anti-tubercular drug design and development [26-28]. A number of studies were performed in the detection and exploration of S315 mutation, and, their implication only [1, 29, 30]. The present study mainly focuses on screening of promising molecules for pharmacologically-relevant chemical libraries of lead-like molecules, fragments or building blocks of Asinex antibacterial chemical library database for identification and optimization to obtain novel katG mutant inhibitors. Further, molecular inhibition mechanisms of identified novel inhibitors were explored rigorously applying *in silico* methods such as molecular docking and dynamics simulations, binding free energy estimations and ADME (absorption, distribution, metabolism, and excretion) predictions. The ADME efficiency of the finally selected five compounds have been determined which indicate good pharmacokinetics and pharmacodynamics profiles, hence, suggested the possibility of being better anti-tubercular drugs in the future.

2. Materials and Methods

2.1 Selection and preparation of molecular database

The Asinex antibacterial chemical library (http://www.asinex.com/antibacterial_compound_library-html/) was chosen for *in-silico* modeling study over the various chemical compounds libraries are freely available for virtual screening. The antibacterial chemical dataset was downloaded in structural

data format (sdf) followed by conversion into a different file format (.pdb and .mol2) with the help of Open Babel [31], an open-source software tool for different molecular file format compatibility. Selected above chemical library comprising of 8044 unique compounds those are developed by Asinex for antibacterial research or virtual screening. Moreover, these compounds are held natural product-like scaffolds with the presence of polar functional groups which can be used for hit-to-lead identification and optimization, fragment-based drug design (FBDD), and SBDD, etc. All selected compounds were prepared in 'LigPrep' wizard of Maestro. Further, all compounds were saved as PDBQT format, as a special file format specifically used in AutoDock Vina [32] tool for future uses. Additionally, long been used drug molecule **INH** has been considered as a control molecule throughout the study also prepared following the same procedure.

2.2 Selection of wild-type(WT) and mutant-type (MT)katG proteins

For the selection of wild-type (WT) x-ray crystal structure of catalase-peroxidase (katG), a search was made in TubercuList database (http://genolist.pasteur.fr/TubercuList/) that in turn gives cross-reference Protein Data Bank (PDB) [33] ID as a result. Based on the availability of structural information and resolution of the crystal structure of the WT katG encoded by *katG* gene of Mtb (strain ATCC 25618 / H37Rv) was retrieved from PDB [PDB ID - 1SJ2], comprising of 743 amino acid residues [34]. In Mtb strain, mutations at codon 315 of the *katG* confer moderate to the high level of resistance to **INH** [35]. Particularly, five different mutant types *viz.* S315T, S315I, S315R, S315N, and S315G were selected for the present study and their models generated using Swiss-PdbViewer [36] by substituting serine residue with respective different mutated amino acid residues. The retrieved 1SJ2 PDB file was considered as the template structure for all mutant PDB structures model generation. All model structures were prepared and optimized using the 'Protein Preparation Wizard' of Maestro [37].

2.3 Molecular docking

Using AutoDock Tool (ADT) v4.2 [38], WT and all MT katG proteins were prepared for docking study. Water molecules were removed from all crystal structures and the appropriate number of polar hydrogen atoms added to the structures. Additionally, Gasteiger charges were assigned to all MT and WT katG protein structures. After completion of protein preparation step, the docking was performed using a grid box of dimension of 40 Å × 40 Å × 40 Å in ADT covering the protein structure with

keeping the center of the binding site coordinates at (45.084, -10.162, 22.978). The grid box, protein, and ligand information were kept inside a config file as in text format for using in ADT [38]. During docking execution, each protein structure was kept as rigid; while all 8044 prepared ligands allowed full flexibility. Autodock vina is installed at Linux based CHPC Lengau server (https://www.chpc.ac.za/index.php/resources/lengau-cluster). On completion the molecular docking of all 8044 antibacterial compounds with WT and all MT katG proteins the results were explored based on the lowest binding affinity score. The binding affinity score of **INH** was considered as a cut-off score for the best active compound selection. Therefore, all protein-ligand complexes were checked critically to screen-out top binding mode conformations having high negative binding affinity score than **INH** and subsequently selected for further modeling analysis. Initially, using the MOE (https://www.chemcomp.com/,V2018), molecular interactions map were observed and protein-ligand contacts analyzed for all complexes, individually. However, for better understanding selected protein-ligand complexes were further visualized in PyMol tool for analyzing different mode of molecular interactions profiles in three-dimensional (3D) space.

2.4 Molecular dynamics (MD) simulation and binding free energy calculation using MM-PBSA (Molecular Mechanics Poisson-Boltzmann Surface Area) method

In order to evaluate the dynamic behavior of proposed inhibitors-katG complexes, the all-atom MD simulation was carried out for 100 ns of time span. The MD simulation was performed in Gromacs 2018.2 (http://www.gromacs.org/) software tool installed at Lengau CHPC server (https://www.chpc.ac.za/index.php/resources/lengau-cluster). SwissParam tool [39] was used to create a topology file of all small molecules. The CHARMM27 atom force field was applied to the system for carrying out the MD simulation. A cubic water box of spc216 water molecules was surrounded to each complex of protein-ligand system. The space between the boundary of the cubic box and any atom of the protein was maintained at a minimum distance of 10Å. To neutralize the system appropriately, suitable numbers of Na^+ and Cl^- ions were utilized added in the system. The neutral system was well equilibrated and minimized by using the steepest descent algorithm 10,000 steps. For long-range interactions, a cutoff range of 0.9 and 1.4 nm were used for van der Waals and electrostatic interactions respectively. At every 1 ps interval the snapshots were recorded and saved for further analyses of each trajectory of MD simulation productions. All atomistic MD simulation was carried out for 100 ns MD production with a time step of 2 fs at the constant pressure of 1 atm

and constant temperature of 300 K. After successful completion of MD simulation, several analyzing parameters included root-mean-square deviation (RMSD), root-mean-square fluctuation (RMSF) and radius of gyration (Rg) were analyzed to check the conformational and performance stability of each molecular complex system in a dynamic environment. The RMSD of protein backbone atoms were calculated based on the atom selection aligned on the reference frame backbone atoms. Followed by the MD simulation the entire trajectories of each system were considered to estimate the binding free energy through MM-PBSA (Molecular Mechanics Poisson-Boltzmann Surface Area) method by the help of g_mmpbsa – Gromacs tool [40]. Details of MM-PBSA procedure can be found in our previous publication [41].

3. Results and discussion

The crystals structure of the katG (PDB ID: 1SJ2) [34] was retrieved from the RCSB-PDB followed by mutation made at Ser315 to generate five MT katG proteins such as MT katG: S315T, MT katG: S315I, MT katG: S315R, MT katG: S315N, and MT katG: S315G. The 3D-structure of all mutant and wildtype KatG are given in Figure S1 (Supplementary data). Detailed flow diagram of the employed work for the current study is portrayed in Figure 1.

3.1 Virtual screening

More than eight thousand molecules from the Asinex database (antibacterial chemical library) were obtained for molecular docking study with WT katG and all MT katG proteins. Further, to identify promising and potential drug-like molecules from the large pool of chemical library showing binding affinity to interacting with selected katG proteins, the molecular docking was performed considering as one of the crucial and pivotal methods used in modern days drug discovery research practice. Entire dataset of antibacterial molecules and including the **INH** were docked using widely utilized molecular docking program Autodock vina. Binding affinity distribution of all 8044 antibacterial compounds docked with five different mutant katG and wild type katG protein are presented in Figure S2. In molecular docking analysis, the binding affinity of **INH** with WT katG protein was found to be - 6.2 Kcal/mol (Table 1). Hence, to narrow down the chemical space of the molecule, cut-off value of binding affinity was considered as -6.20 Kcal/mol. The binding affinity of all docked molecules from both wild and mutant types was explored. Molecules succeeded in the above criteria (binding energy ≤ -6.2 Kcal/mol) from all WT and MT were merged. After deletion of duplicates

from merged molecules, finally altogether 4456 molecules retained, thus accounted for further screening.

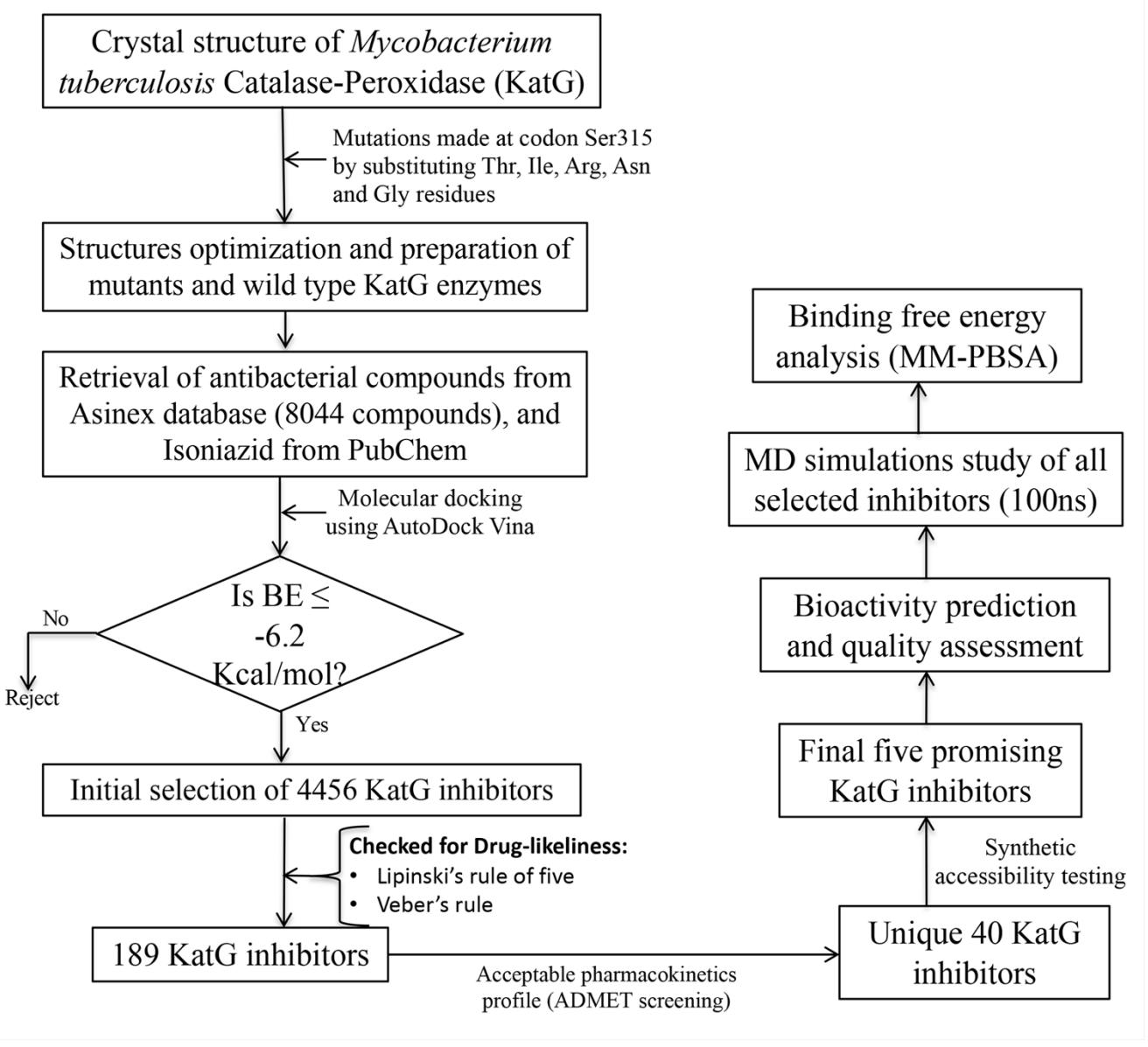

Figure 1. Flow diagram of screening and designing of katG inhibitors

Further, the Lipinski's rule of five (RO5) [42] and Veber's rule [43] were checked for all 4456 molecules obtained from the previous step. More precisely, RO5 implies prediction or identification of drug-like pharmacological properties of molecules applied to drug discovery research to prioritize molecules with an increased likelihood of good oral absorption or permeation. Lipinski's RO5 states

that an orally active compound or drug candidate should have the following parameters such as hydrogen bond donors ≤ 5, hydrogen bond acceptors ≤ 10, molecular weight ≤ 500, and an octanol-water partition coefficient (logp) value < 5. On the other hand, Veber's rule implies that compounds will show good oral bioavailability when candidate obey the following criteria such as rotatable bonds (ROTB) and polar surface area (PSA) less than 10 and 140 $Å^2$ respectively. Total 4267 molecules were failed to pass both rules and subsequently remaining 189 compounds taken for *in-silico* pharmacokinetics study. In the ADME analysis, 149 molecules failed to show acceptable pharmacokinetics profile (i.e. they are not displaying high GI absorption, or not exhibiting good solubility and skin or blood-brain barrier permeability profiles) and therefore removed from further analysis. Finally, the synthetic accessibility [44] of the remaining 40 molecules was checked. Distribution of synthetic accessibility values of 40 compounds is given in Figure S3 (Supplementary data). It is illustrated that high synthetic accessibility value indicates the difficulty to synthesize, hence low synthetic value always recommended in pharmaceutical and medicinal chemistry research. In our analysis, synthetic accessibility of five molecules was found to be less than 5 and conceived as potentially strong interacting molecules for exhibiting inhibitory action against mutant katG protein. Two-dimensional representation of finally selected 5 molecules (**L1**, **L2**, **L3**, **L4**, and **L5**) are given in Figure 2.

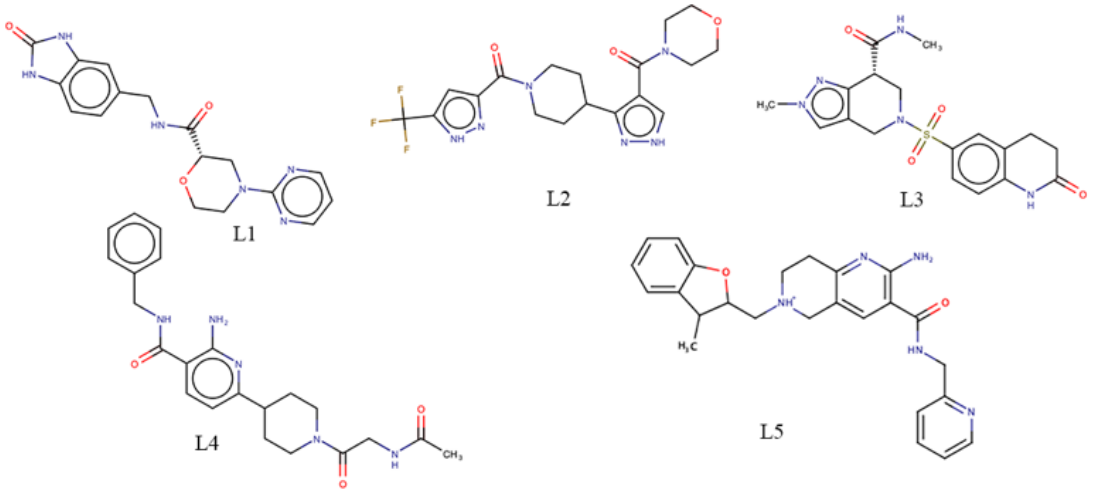

Figure 2. Two-dimensional representation of final screened mutant katG inhibitors

3.2 Molecular docking and binding interactions analysis

The binding affinity of all five promising molecules and **INH** towards all mutants and WT katG was rigorously explored for molecular interaction analysis and results presented in Table 1. On a detailed analysis of binding affinity, it can be seen that all proposed molecules showed a strong affinity towards WT and MT katG enzyme in comparison to the **INH**. It is also interesting to observe that all proposed molecules except **L2** were found to give higher binding energy when docked to the MT katG. The binding energy of **L2** with WT katG and MT katG was found to be comparable. From Table 1, it can also be observed that the binding affinity of all proposed molecules (**L1**, **L2**, **L3**, **L4**, and **L5**) found to be the higher when docked with S315R in comparison to WT katG and other MT katG proteins. Hence, in subsequent analysis, the binding interactions and all atom-based MD simulation study were performed for selected protein-ligand complexes between proposed molecules and MT katG: S315R. Two-dimensional representation of best-docked conformation of each of the final proposed molecules (Figure 2) and **INH** with MT katG: S315R are displayed in Figure 3.

Table 1: Binding energy of the final proposed katG inhibitors and **INH**

Molecule	Binding energy (Kcal/mol)					
	katG: WT	Mutant katG				
		S315T	S315I	S315R	S315N	S315G
INH	-6.20	-5.80	-5.70	-6.10	-5.90	-5.70
L1	-8.00	-8.10	-8.70	-8.90	-8.50	-8.30
L2	-8.20	-8.30	-8.20	-8.50	-8.20	-8.20
L3	-7.80	-7.90	-8.10	-8.40	-8.10	-7.70
L4	-8.40	-8.80	-9.00	-9.20	-8.80	-8.60
L5	-7.90	-8.00	-8.30	-8.40	-8.00	-8.00

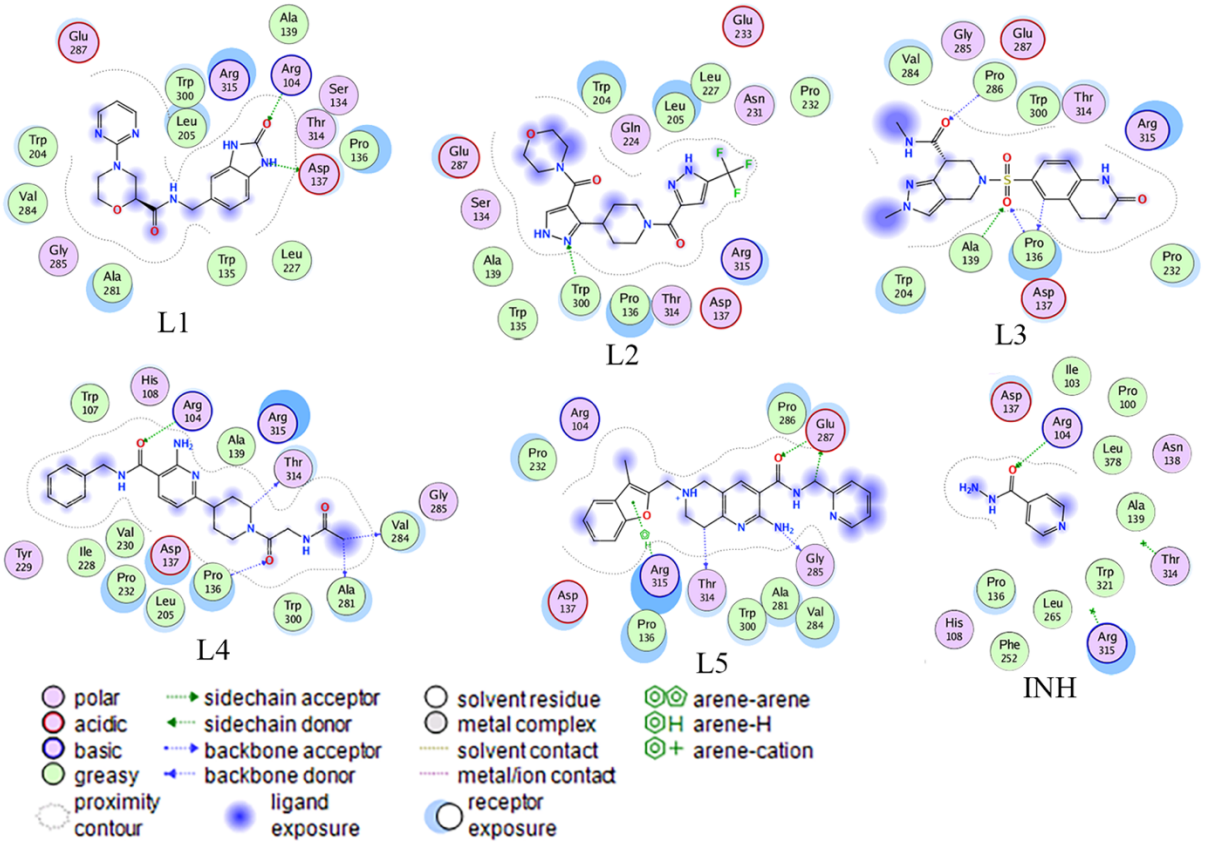

Figure 3. Binding interactions potentialities between finally selected 5 inhibitors and MT katG: S315R in 2D representation

From Figure 3, it can be ascertained that Arg315 (mutated amino residue) directly interacted with **L5**, for other molecules, Arg315 was found to be in the close proximity or vicinity of the receptor cavity which might indicate that structural or conformational changes of molecules can form binding interaction with the same. Arg104 and Asp137 were found to be crucial to form hydrogen bond (HB) interactions with both **L1** and **INH** molecules. Both **L3** and **L4** clashed with Pro136 through HB interactions. Two residues, Ala139 and Pro286 were found to be crucial to interact with **L3**. Figure 3 indicated that Ala282, Val284, and Arg304 were successfully established binding interactions with **L4**. On the other hand, **L2** was able to connect with Trp300 through HB interactions. Gly285 and Glu287 were critical to form interaction with **L5**. Beyond above mentioned participating amino acid residues and interactions, a number of other crucial amino residues were found around the proposed promising molecules. In an earlier study by Lingaraja Jena et al., was reported that docking analysis of WT-katG protein with **INH** have yielded the binding energy score of -5.36 kcal/mol, where as in

the present study the docking analysis of WT-katG protein with **INH** binding energy score observed as -6.20 kcal/mol. Furthermore, the same study was also reported **INH** docking analysis with two mutant types i.e. S315T and S315N, the binding energy found to be -4.98 and -5.15 kcal/mol, respectively [27]. The binding energy of **INH** in the present study was found to be -5.80 and -5.90 kcal/mol for S315T and S315N, respectively. In another study, **INH** was shown the highest binding interaction affinity with MT-S315G katG than the WT-katG, and followed by MT-S315I, MT-S315T and MT-S315N [28]. In addition to the above mentioned findings, Strivastava et al., were also reported similar kind of docking interaction profiles when **INH** docked with MT-katG S315T protein [45]. In the above study, authors were able to show that amino acid residues Arg104 and Asp137 of MT-katG S315T protein interacted with **INH**. In our study, molecular docking analysis revealed similar kind of molecular interaction profiles for screened compounds. More interestingly, among the five finally proposed katG inhibitors, **L1** and **L4** were found to form alike H-bond interactions profile with the MT-KatG protein. Another important residue Asn137 was also found be in close proximity of the binding site for forming molecular interaction with the all five selected katG inhibitors. Binding mode of all proposed molecules in surface view representations with the MT katG: S315R is given in Figure 4. From Figure 4, it is clearly visible that all molecules perfectly organized and fitted inside the receptor cavity of MT katG: S315R. Therefore, molecular docking analysis distinctly explained that all proposed molecules would be extensively promising to inhibit the MT katG. It is also crucial to note that the binding affinity of **INH** reduces when it binds to the MT katG but the proposed molecules showed enhanced binding affinity towards the MT katG. The above observations undoubtedly explained that proposed molecules hold specific chemical characteristics for expressing strong potentiality to inhibit the MT katG and can address to manage the drug-resistant issue in the treatment of TB.

Taken together, it can be suggested that plausible inhibitory mechanism of the newly identified potential chemical entities lies on their specific chemical structural features such as compound **L1** holds carbonyl and amine groups participated to form strong intermolecular interaction with active site residues of mutant katG protein. Likewise, compound **L1**, compounds **L3**, **L4** and **L5** have also shown similar interaction mechanisms for inhibiting the mutant katG activity. Additionally, these three compounds (**L3, L4** and **L5**) hold molecular interactions with other carbon atom and methyl group to hold sufficiently strong and potential interaction profiles as inhibitory mechanism. Identified compound **L2**, although hold various functional groups containing F, N, O atoms, but only nitrogen

atom interacted with residue Trp300 to show molecular interaction and hence exhibiting inhibitory mechanism. Whereas, for the standard drug **INH**, it has been earlier illustrated that KatG oxidatively activates the **INH** to inhibits Mtb cell wall lipid synthesis by interacting or producing a range of oxygen-, nitrogen- and carbon-centered free radical species [46]. From the interaction profiles of the newly identified katG mutant inhibitors it can be clearly observed a greater number of molecular interactions as compared to the **INH**. This is probably due to the comparatively less or minimum numbers of hydrogen-bond acceptors and hydrogen-bond donors atoms present in **INH** as compared to the newly identified compounds. Hence, it can be postulated that the proposed katG inhibitors possess higher or comparable inhibitory mechanism as **INH** towards the katG protein.

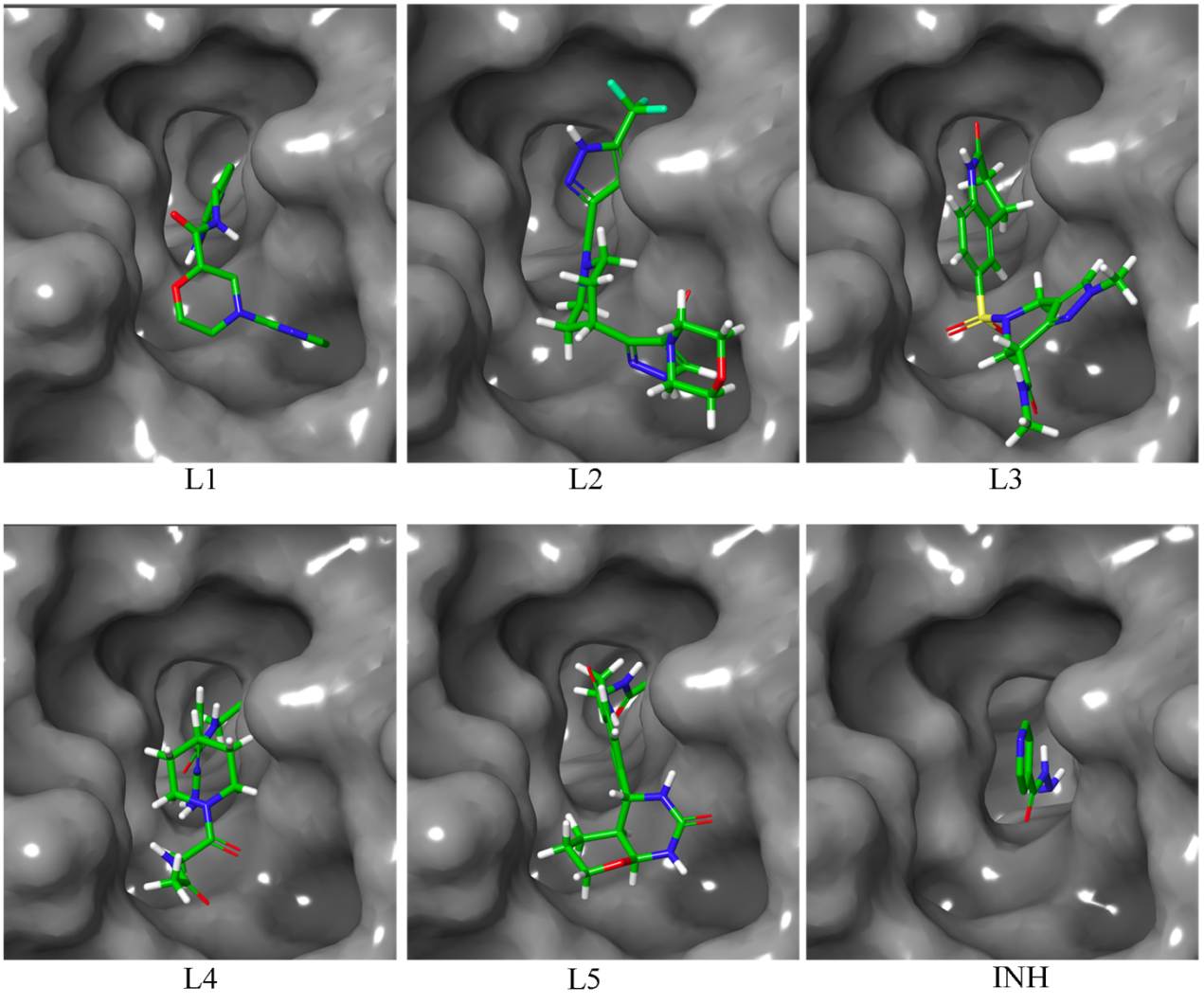

Figure 4. Binding pose of proposed katG inhibitors and **INH** in 3D surface view orientation.

3.3 Quality assessment of proposed molecules

Pharmacokinetics and physicochemical properties analyses of any given chemical substance can explain the potentiality of the chemical substance to reach the active site with therapeutic concentration. Therefore, all proposed molecules (**L1**, **L2**, **L3**, **L4**, and **L5**) were considered for *in-silico* pharmacokinetics and physicochemical analyses. Different important pharmacokinetics and physicochemical parameters including the lipophilicity were obtained from the online tool SwissADME (http://www.swissadme.ch/) and values are presented in Table 2. The range of molecular weight of all molecules was found between 350 to 431 g/mol. Polar surface area can give an idea about the orally active characteristics of the molecule. For molecule **L1**, **L2**, **L3**, **L4,** and **L5** the polar surface area was found to be 116.00, 107.21, 121.78, 117.42 and 94.57 $Å^2$ respectively which undoubtedly indicated that all molecules are orally active in nature. Except for molecule **L5**, all molecules were found to be moderately or highly soluble in nature. Most importantly, gastrointestinal absorption (GI) parameter comes out with high value for all molecules indicates easily and highly absorbable in the intestine. Additionally, apparently low synthetic accessibility of all molecules evidently suggested that none of the molecules is difficult to synthesize.

Table 2. Physicochemical parameters of selected katG inhibitors.

Parameters	**L1**	**L2**	**L3**	**L4**	**L5**
Formula	$C_{17}H_{18}N_6O_3$	$C_{18}H_{21}F_3N_6O_3$	$C_{18}H_{21}N_5O_4S$	$C_{22}H_{27}N_5O_3$	$C_{25}H_{28}N_5O_2$
[1]MW (g/mol)	354.36	426.39	403.46	409.48	430.52
[2]NHA	26	30	28	30	32
[3]NAHA	15	10	11	12	18
[4]NRB	5	6	4	9	6
[5]MR	97.34	104.21	108.26	117.42	127.60
[6]TPSA (Å²)	116.00	107.21	121.78	117.42	94.57
[7]LogS	-4.91	-3.95	-4.25	-5.74	-7.42
[8]SC	Very soluble	Soluble	Very soluble	Moderately soluble	Poorly soluble
[9]GI	High	High	High	High	High
[10]vROF	0	0	0	0	0
[11]BS	0.55	0.55	0.55	0.55	0.55
[12]SA	3.01	3.61	3.79	2.99	4.16
LogP	1.69	1.49	2.07	2.62	3.41

[1]Molecular weight; [2]No. of heavy atoms; [3]No. of aromatic heavy atoms; [4]No. of rotatable bonds; [5]Molar refractivity; [6]Topological polar surface area; [7]Solubility; [8]Solubility class; [9]Gastrointestinal absorption; [10]Violation of Lipinski's rule of five; [11]Bioavailability Score; [12]Synthetic accessibility

The graphical representation of drug-likeness properties of the molecules can be viewed in bioavailability radar plot for better understanding. For all five proposed molecules bioavailability radar plot obtained from SwissADME and given in Figure 5. Different properties of the molecule included unsaturation (INSATU), insolubility (INSOLU), hydrophobicity (LIPO), rotatable bonds (FLEXI), molecular weight (SIZE) and polar surface area (POLAR) are represented by the pink area. It is illustrated that recommended value of different parameters are -0.7 < LIPO < +5, SIZE < 500g/mol, 20 $Å^2$ < POLAR < 130 $Å^2$, 0 < INSOLU < 6, 0.25 < INSATU < 1, and 0 < FLEX < 9 for drug-like molecules. The radar plots of the proposed molecules clearly enlightened that all compounds possess acceptable drug-likeliness characteristics.

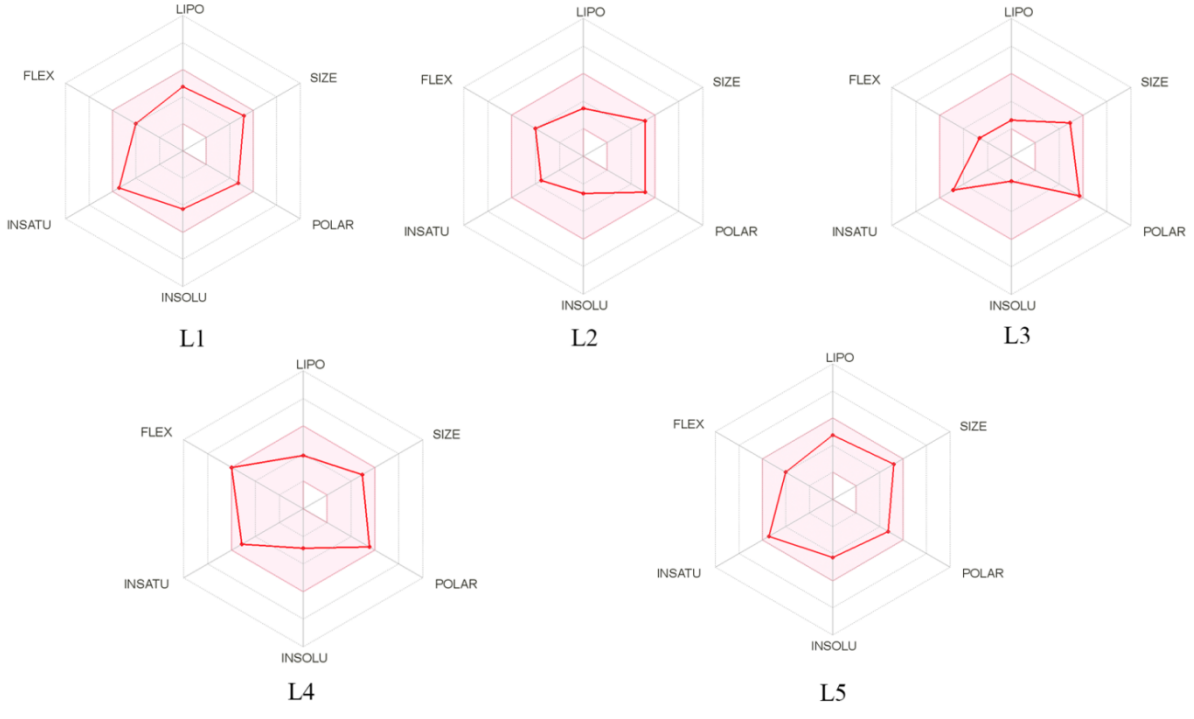

Figure 5. Bioavailability radar plot for the final katG inhibitors

Further, the human intestinal absorption (HIA) and blood-brain barrier (BBB) were explored using the egg-boiled model portrayed in Figure 6. In the egg-boiled model, a molecule can be considered to possess high HIA penetration if it belongs to the white region (albumin). Conversely, a molecule present in the yellow region (yolk) indicates high BBB penetration. Both white and yellow regions in the egg-boiled model are not mutually exclusive. All five molecules were found in the albumin area

suggested good absorption in the HIA. Most importantly none of the molecules was found to be outside the boiled-egg region. Another parameter, substrates (PGP+) and non-substrates (PGP-) of the permeability glycoprotein (PGP) are indicated with blue and red color circles correspond to the egg-boiled model. The PGP decreases the efficiency of PGP+ molecule due to pushes them back into the intestinal lumen in the liver. Therefore, egg-boiled model (Figure 6) illustrated that all molecules are in the category of PGP+ hence they belong to the substrate. From above pharmacokinetics and physicochemical parameters analyses significantly explained that all proposed molecules possess enough potential to be drug-like characteristics.

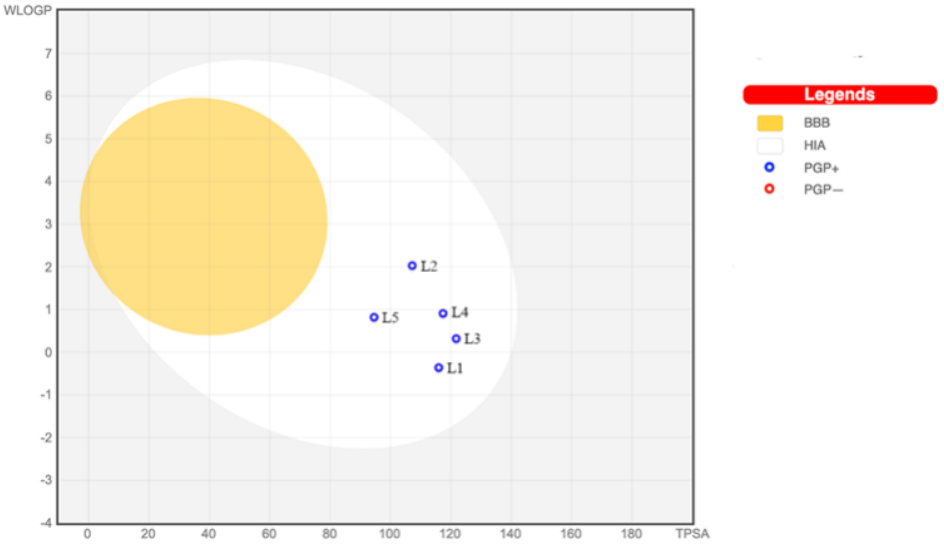

Figure 6. The EGG-BOILED model for the final screened katG inhibitors

3.4 Bioactivity prediction and quality assessment

The binding energy obtained from molecular docking study performed in AutoDock vina was used to calculate the inhibitory constant (K_i) of the final selected molecules along with ligand efficiency (LE), LE scale (LE_{scale}), fit quality (FQ) and LE-dependent lipophilicity (LELP). All analyzed parameters are given in Table 3.

The following equation (1) [47] was used to calculate the K_i (μM) in which R represents as the gas constant (1.987×10^{-3}kcal/K-mol)) and T (298.15 K) represents to the absolute temperature of the protein-ligand complex.

$$K_i = e^{\frac{-\Delta G}{RT}} \qquad (1)$$

According to the K_i value in Table 3, proposed katG inhibitors can be arranged with their potentiality as **L4**, **L1**, **L2**, **L3**, and **L5**. The low K_i value of all molecules strongly favors being lead molecules with high potency [48, 49].

Another parameter, LE can be used to check lead-likeness of the molecules and which recommended by Hopkins *et al*.[50]. The LE can be calculated by the negative ratio between binding energy and the number of heavy atoms (Equation 2). All proposed molecules showed the LE value less than 0.350 that indicated as a lead-like molecule.

$$LE = \frac{-BE}{NHA} \tag{2}$$

According to Reynolds *et al*. [51], the LE parameter is unable to calculate without molecular size. They have proposed the LE scaling (LE_Scale) which is a size-independent comparison of ligands and can be calculated using equation (3). The LE_Scale of all proposed molecules was calculated and given in Table 3. A low value (less than 0.4) of LE_Scaled effusively suggested that proposed molecules might be potential katG inhibitors.

$$LE\_Scale = 0.873 \times e^{-0.026 \times NHA} - 0.064 \tag{3}$$

Table 3. Bioactivity and efficiency parameters of proposed katG inhibitors

Molecule	[1]BE	[2]K_i (μM)	[3]LE	[4]LE_Scale	[5]FQ	[6]LELP
L1	-8.90	0.295	0.342	0.380	0.900	4.942
L2	-8.50	0.581	0.283	0.336	0.842	5.265
L3	-8.40	0.688	0.300	0.358	0.838	6.900
L4	-9.20	0.178	0.307	0.336	0.914	8.534
L5	-8.40	0.688	0.263	0.316	0.832	10.791

[1]Binding energy; [2]Predicted inhibition constant; [3]Ligand efficiency; [4]Ligand efficiency scale; [5]Fit quality; [6] ligand-efficiency-dependent lipophilicity

Equation 4 was used to calculate the fit quality (FQ) which is the ratio of LE and LE_Scale. The value of FQ near 1 explain good binding to the receptor [52]. Not a single molecule was found to have FQ value less than 0.830 (Table 3) which undoubtedly explained that molecules efficient enough to perfect binding to the studied katG protein.

$$FQ = \frac{LE}{LE\_Scale} \tag{4}$$

Keseru and Makara [53] proposed another important parameter, ligand-efficiency-dependent lipophilicity (LELP) which can be obtained by dividing the logP value by LE (Equation 5). It is illustrated that being a lead-like molecule LELP should be > **3** [52]. LELP value of all proposed katG inhibitors was calculated and given in Table 3. High LELP value definitely suggested that molecules optimized the affinity with respect to lipophilicity.

$$LELP = \frac{\log p}{LE} \tag{5}$$

3.5 Molecular dynamics

The dynamic behavior of the complex of each protein-bound molecules was explored through a long range up to 100 ns MD simulation study. Several analyzing parameters included RMSD, RMSF and Rg were explored to analyze the relative stability of the simulated complexes. From start to end MD simulated trajectories were used to calculate the protein backbone RMSD and plotted against simulation time (Figure 7). In Figure 7, it can be observed that all trajectories were substantially equilibrated during the simulation phase except the protein-bound with **L4** molecule. The protein backbone of the complex of **L4** was shown stability up to about 30 ns of simulation time. Afterward, RMSD was started increasing and finally showed stability. For each simulated complex, average, maximum and minimum RMSD values were calculated and given in Table 4. Difference between maximum and minimum RMSD values were found to be 0.329, 0.318, 0.340, 0.560, 0.372 and 0.330 nm for **L1**, **L2**, **L3**, **L4**, **L5**, and **INH** respectively. This low difference suggests that all MD simulations have been substantially equilibrated. Small differences or changes observed in RMSD in the order of 1-3 nm which undoubtedly suggested that selected katG inhibitors bound protein complexes not underwent for any noticeable structural or conformational changes throughout the simulation run.

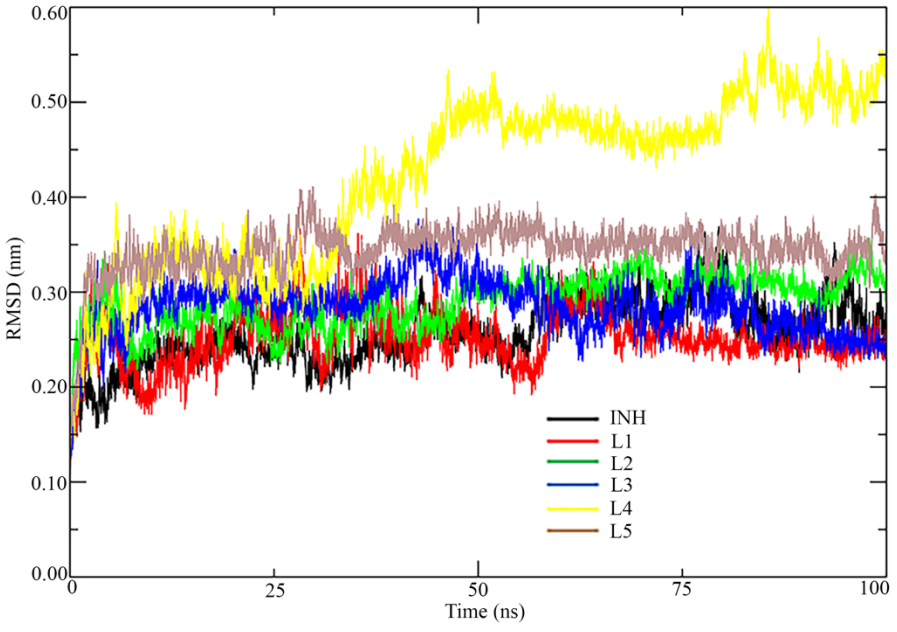

Figure 7. RMSD vs time of katG backbone obtained from complexes of katG-screened inhibitors and katG-INH

In addition to RMSD of the protein backbone, the ligand RMSD was also estimated which found to be very low for all ligands. The average value of ligand RMSD was found as 0.194, 0.192, 0.098, 0.192, 0.155 and 0.082 nm for **L1**, **L2**, **L3**, **L4**, **L5**, and **INH,** respectively. Ligand's maximum and minimum RMSD values were found to be 0.300 and 0.001; 0.326 and 0.0005; 0.291 and 0.0005; 0.301 and 0.0005; 0.239 and 0.0005; and, 0.140 and 0.0005 nm for **L1**, **L2**, **L3**, **L4**, **L5**, and **INH,** respectively. The RMSD vs time of the simulation plot of all ligands is given in Figure S4 (Supplementary file).

Individual amino residue plays a critical role in the stability of the molecule inside the receptor cavity. The RMSF value of each amino acids was calculated and given in Figure 8. Average, maximum and minimum RMSF values of all complexes were calculated and given in Table 4. From Figure 8, it was also observed that amino acids present at the amine terminal region of the sequence fluctuated about 1.50 nm but remaining amino residues were not attended much deviation. Average RMSF can give an idea about the fluctuation of the amino acid of the protein molecule. Mean RMSF was found to be 0.158, 0.161, 0.150, 0.163, 0.136, and 0.131 nm for **L1**, **L2**, **L3**, **L4**, **L5**, and **INH** respectively. Moreover, the average value of ligand RMSF was estimated and found to be as 0.118, 0.107, 0.106, 0.158, 0.072 and 0.078 nm for **L1**, **L2**, **L3**, **L4**, **L5**, and **INH,** respectively. Difference

between maximum and minimum RMSF value of ligand was found to be 0.199, 0.160, 0.213, 0.293, 0.151 and 0.150 nm for **L1**, **L2**, **L3**, **L4**, **L5**, and **INH,** respectively. No doubt, the above RMSD and RMSF values of ligand and protein, suggest that all ligand were stable enough in a dynamic environment and hence suggesting ligand stability inside the binding pocket of katG.

Table 4: Maximum, minimum and average value RMSD, RMSF and radius of gyration (Rg) of final proposed molecules

Complex	RMSD			RMSF			Rg		
	[1]Max.	[2]Min.	[3]Avg.	[1]Max.	[2]Min.	[3]Avg.	[1]Max.	[2]Min.	[3]Avg.
L1	0.367	0.038	0.251	1.305	0.060	0.158	2.939	2.791	2.864
L2	0.357	0.039	0.284	1.075	0.057	0.161	2.915	2.813	2.863
L3	0.377	0.037	0.284	1.084	0.053	0.150	2.921	2.812	2.867
L4	0.599	0.039	0.422	1.642	0.0632	0.163	2.948	2.816	2.884
L5	0.411	0.039	0.344	0.633	0.052	0.136	2.900	2.813	2.865
Isoniazid	0.369	0.039	0.256	1.191	0.050	0.131	2.935	2.810	2.865

[1]Maximum; [2]Minimum; [3]Average

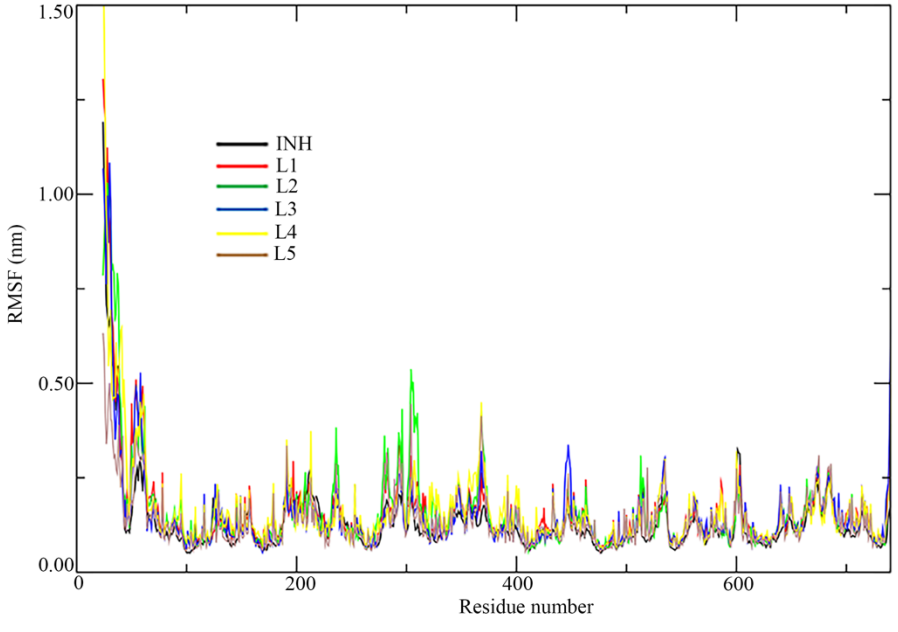

Figure 8. RMSF vs residue number of katG when bound to final screened katG inhibitors and **INH**

Moreover, the Rg fluctuations of the studied protein-ligand complexes can be explained by Rg parameter obtained from the MD simulation trajectories. Rg values of all proposed molecules along

with **INH** were recorded and portrayed in Figure 9. Trajectories of Rg explained without any doubt that all system remains rigid during the simulation. Maximum, minimum and average Rg values are given in Table 4. Difference between maximum and minimum Rg can give a clear picture about the fluctuation of the system during the MD simulation. The differences in Rg i.e. value of (Maximum Rg – Minimum Rg) was found to be 0.148, 0.102, 0.109, 0.132, 0.087 and 0.125 nm for **L1**, **L2**, **L3**, **L4**, **L5**, and **INH,** respectively which clearly explained the rigidity of the systems. Hence, detailed exploration of RMSD, RMSF and Rg values of all the MD simulated systems suggested that all proposed molecules can form a dynamically stable complex with katG enzyme.

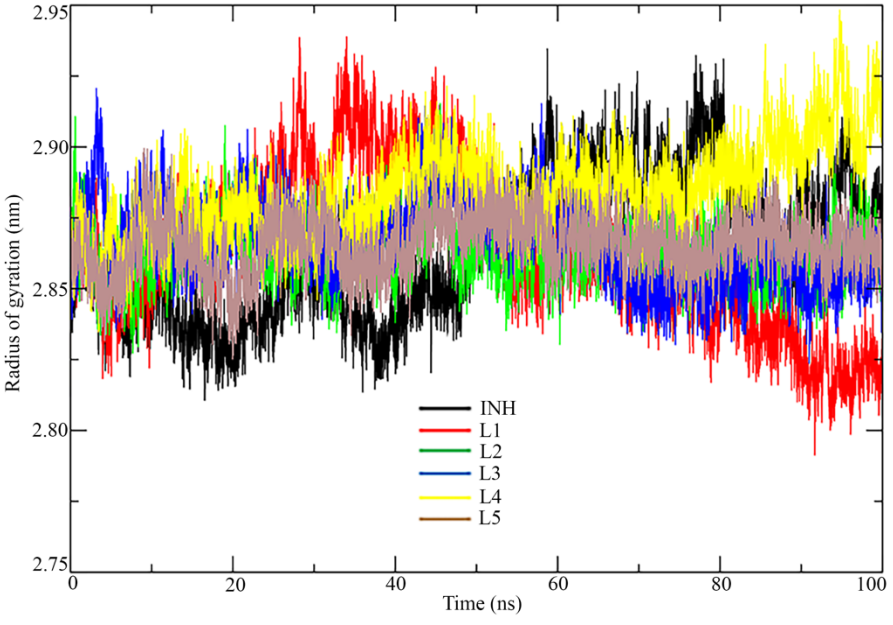

Figure 9. Radius of gyration vs time obtained from complexes of katG-screened inhibitors and katG-**INH**

3.6 Binding free energy analysis using MM-PBSA method

To calculate the binding free energy from MD simulation trajectory of proposed ligands along with **INH**, the MM-PBSA method was used. The binding free energy against the time of the simulation of all complexes was plotted and given in Figure 10. The average value of binding free energy was found to be -198.117, -180.166, -184.150, -217.446, -201.833, and –156.338 Kcal/mol for **L1**, **L2**, **L3**, **L4**, **L5**, and **INH** respectively. In Table 5, the MM-PBSA based estimated binding free energies of the corresponding protein-ligand complexes over 100000 trajectories during the MD production period of 100 ns are presented along with the standard error. From the above data and Figure 10, it

was observed that the binding free energy of all final proposed molecules better than **INH**. Srivastava et. al., have reported binding free energy values calculated using MM-PBSA method for MT-S315T katG proteins, however, the study has found weak binding energy of -33.307 kJ/mol in the binding site-1 [45]. Therefore, it is undoubtedly clear that final selected molecules might have a strong binding affinity towards the studied katG.

Table 5: MM-PBSA based binding free energies (kcal/mol) with standard error of mean of finally selected five protein-ligand complexes and INH-katG complex.

Complex	MM-PBSA based binding free energies (kcal/mol)		
	[1]Max.	[2]Min.	[3]Avg. / Standard error
L1	-100.798	-262.224	-198.117 ± 0.261
L2	-90.63	-257.098	-180.166 ± 0.253
L3	-117.735	-240.853	-184.150 ± 0.155
L4	-166.876	-331.601	-217.446 ± 0.251
L5	-176.06	-301.969	-201.833 ± 0.161
Isoniazid	-128.811	-176.081	-156.338 ± 0.085

[1]Maximum; [2]Minimum; [3]Average

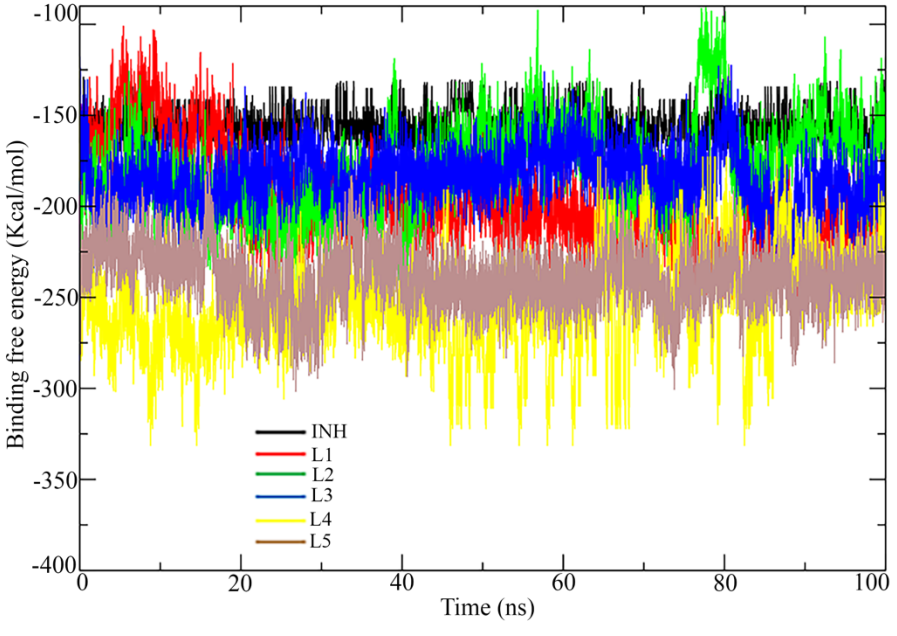

Figure 10. Binding free energies towards katG of final proposed katG inhibitors and **INH.**

4. Future perspectives

Traditional drug discovery approach is extensively time and resource-consuming as well as expensive method. In this situation, pharmacoinformatics approaches such as virtual screening, molecular docking, and MD simulations became effective and pivotal tools in modern drug discovery research. Although the application of pharmacoinformatics methods in drug development is faster and cheaper but there is still a need for experimental validation for further confirmation. Herein, aiming towards the identification of potential anti-tubercular drug-like candidate molecules proposed as katG inhibitors employing advanced pharmacoinformatics approaches need further experimental validations by means of *in vitro* and *in vivo* studies to confirm as lead molecules before stepping into clinical trials. Binding affinity can be verified using thermal-melt assays and subsequently by physiological functions against the bacteria - Mtb. Furthermore, experimental approaches can be adopted to explore the binding and non-binding events or the drug-protein residence time can be implemented for a good experiment-based understanding of the inhibitory activity of the final proposed katG molecules [54].

5. Conclusion

Five different mutant katG enzyme crystal structures were generated by replacing Ser315 by drug-resistance causing mutant amino acid residues *viz.* Thr, Ile, Arg, Asn, and Gly. More than eight thousand antibacterial molecules were collected from Asinex database and molecular docking based virtual screening was performed with all mutant and wild type katG enzyme. All docked compounds were screened out by comparing the binding energy of **INH** followed by RO5, Veber's rule, ADME profile, and synthetic accessibility parameters. Finally, five molecules were found to be promising and potential against the katG enzyme and being important antibacterial chemical agents. Molecular docking study demonstrated a number of binding interactions with catalytic amino residues of the katG. Various pharmacokinetics parameters of the proposed molecules favor the good absorption, distribution, and penetration to the HIA. Predicted low inhibitory constant (K_i) value undoubtedly explain that molecules are potential inhibitors. The quality of the molecules was assessed using several parameters including ligand efficiency, ligand efficiency scale, fit quality, and ligand-efficiency-dependent lipophilicity. Value of the above parameters substantiated in favor of the lead like molecules. The dynamic behavior of both protein and proposed molecules was checked through a

100ns MD simulation study. The RMSD, RMSF, and Rg values were calculated from the MD simulation trajectories and clearly suggested all complexes were equilibrated in nature. Finally, the affinity of the proposed molecules was checked through the binding free energy calculation using the MM-PBSA approach. The negative binding energy was found in both molecular docking and MM-PBSA methods which undoubtedly explained that all proposed molecule are efficient enough to form strong binding interactions with the katG enzyme. Hence, it can be concluded that proposed molecules might be potent and safer lead-like chemical agents for the treatment of bacterial infection subjected to confirmation through experimental studies.

Acknowledgment

This research was funded by the Deanship of Scientific Research at Princess Nourah bint Abdulrahman University through the Fast-track Research Funding Program

Computational resource

The CHPC (www.chpc.ac.za) is thankfully acknowledged for computational resources and tools.

Conflict of interest

Authors declare that there is no competing interest

References

[1] V.R. Bollela, E.I. Namburete, C.S. Feliciano, D. Macheque, L.H. Harrison, J.A. Caminero, The international journal of tuberculosis and lung disease : the official journal of the International Union against Tuberculosis and Lung Disease, 20 (2016) 1099-1104.
[2] S. Portelli, J.E. Phelan, D.B. Ascher, T.G. Clark, N. Furnham, Scientific reports, 8 (2018) 15356.
[3] W.H. Organization, in, 2018.
[4] M.A. Islam, T.S. Pillay, Chemical biology & drug design, 90 (2017) 282-296.
[5] N. Dookie, S. Rambaran, N. Padayatchi, S. Mahomed, K. Naidoo, The Journal of antimicrobial chemotherapy, 73 (2018) 1138-1151.
[6] M. Seifert, D. Catanzaro, A. Catanzaro, T.C. Rodwell, PloS one, 10 (2015) e0119628.
[7] F.A. de Freitas, V. Bernardo, M.K. Gomgnimbou, C. Sola, H.R. Siqueira, M.A. Pereira, F.C. Fandinho, H.M. Gomes, M.E. Araujo, P.N. Suffys, E.A. Marques, R.M. Albano, PloS one, 9 (2014) e104100.
[8] F. Coll, J. Phelan, G.A. Hill-Cawthorne, M.B. Nair, K. Mallard, S. Ali, A.M. Abdallah, S. Alghamdi, M. Alsomali, A.O. Ahmed, S. Portelli, Y. Oppong, A. Alves, T.B. Bessa, S. Campino, M. Caws, A. Chatterjee, A.C. Crampin, K. Dheda, N. Furnham, J.R. Glynn, L. Grandjean, D. Minh Ha, R. Hasan, Z. Hasan, M.L. Hibberd, M. Joloba, E.C. Jones-López, T. Matsumoto, A. Miranda, D.J. Moore, N. Mocillo, S. Panaiotov, J. Parkhill, C. Penha, J. Perdigão, I. Portugal, Z. Rchiad, J.

Robledo, P. Sheen, N.T. Shesha, F.A. Sirgel, C. Sola, E. Oliveira Sousa, E.M. Streicher, P.V. Helden, M. Viveiros, R.M. Warren, R. McNerney, A. Pain, T.G. Clark, Nature Genetics, 50 (2018) 307-316.
[9] A.N. Unissa, C.G. Doss, T. Kumar, S. Sukumar, A.R. Lakshmi, L.E. Hanna, Journal of global antimicrobial resistance, 15 (2018) 111-120.
[10] A.N. Unissa, C.G. Doss, T. Kumar, S. Swathi, A.R. Lakshmi, L.E. Hanna, Journal of global antimicrobial resistance, 11 (2017) 57-67.
[11] T. Jagielski, M. Grzeszczuk, M. Kaminski, K. Roeske, A. Napiorkowska, R. Stachowiak, E. Augustynowicz-Kopec, Z. Zwolska, J. Bielecki, Pneumonologia i alergologia polska, 81 (2013) 298-307.
[12] G. Ramasubban, K.L. Therese, U. Vetrivel, M. Sivashanmugam, P. Rajan, R. Sridhar, H.N. Madhavan, N. Meenakshi, International journal of antimicrobial agents, 37 (2011) 368-372.
[13] M.A. Islam, T.S. Pillay, Journal of biomolecular structure & dynamics, (2019) 1-12.
[14] M.W. Marney, R.P. Metzger, D. Hecht, F. Valafar, Tuberculosis, 108 (2018) 155-162.
[15] M. Jagadeb, S.N. Rath, A. Sonawane, Journal of biomolecular structure & dynamics, (2018) 1-11.
[16] M.A. Isa, R.S. Majumdhar, S. Haider, Journal of molecular modeling, 24 (2018) 132.
[17] R. Dharra, S. Talwar, Y. Singh, R. Gupta, J.D. Cirillo, A.K. Pandey, M. Kulharia, P.K. Mehta, PloS one, 12 (2017) e0183060.
[18] S. Appunni, P.M. Rajisha, M. Rubens, S. Chandana, H.N. Singh, V. Swarup, Computational biology and chemistry, 67 (2017) 200-204.
[19] U.A. More, S.D. Joshi, T.M. Aminabhavi, V.H. Kulkarni, A.M. Badiger, C. Lherbet, European journal of medicinal chemistry, 94 (2015) 317-339.
[20] R. Mehra, R. Chib, G. Munagala, K.R. Yempalla, I.A. Khan, P.P. Singh, F.G. Khan, A. Nargotra, Molecular diversity, 19 (2015) 1003-1019.
[21] S.D. Joshi, U.A. More, D. Koli, M.S. Kulkarni, M.N. Nadagouda, T.M. Aminabhavi, Bioorganic chemistry, 59 (2015) 151-167.
[22] W. Hong, Y. Wang, Z. Chang, Y. Yang, J. Pu, T. Sun, S. Kaur, J.C. Sacchettini, H. Jung, W. Lin Wong, L. Fah Yap, Y. Fong Ngeow, I.C. Paterson, H. Wang, Scientific reports, 5 (2015) 15328.
[23] K.V. Shivakumar, P. Karunakar, J. Chatterjee, Interdisciplinary sciences, computational life sciences, 6 (2014) 292-299.
[24] Y. Maharaj, M.E. Soliman, Chemical biology & drug design, 82 (2013) 205-215.
[25] X.Y. Lu, Y.D. Chen, Y.J. Jiang, Q.D. You, European journal of medicinal chemistry, 44 (2009) 3718-3730.
[26] C.E. Cade, A.C. Dlouhy, K.F. Medzihradszky, S.P. Salas-Castillo, R.A. Ghiladi, Protein science : a publication of the Protein Society, 19 (2010) 458-474.
[27] L. Jena, P. Waghmare, S. Kashikar, S. Kumar, B. Harinath, International Journal of Mycobacteriology, 3 (2014) 276-282.
[28] A.N. Unissa, G.P. Doss C, T. Kumar, S. Sukumar, A.R. Lakshmi, L.E. Hanna, Journal of Global Antimicrobial Resistance, 15 (2018) 111-120.
[29] H. Ando, Y. Kondo, T. Suetake, E. Toyota, S. Kato, T. Mori, T. Kirikae, Antimicrobial Agents and Chemotherapy, 54 (2010) 1793-1799.
[30] A.N. Unissa, N. Selvakumar, S. Narayanan, C. Suganthi, L.E. Hanna, BioMed Research International, 2015 (2015) 5.
[31] N.M. O'Boyle, M. Banck, C.A. James, C. Morley, T. Vandermeersch, G.R. Hutchison, J Cheminform, 3 (2011) 33.
[32] O. Trott, A.J. Olson, J Comput Chem, 31 (2010) 455-461.

[33] H.M. Berman, J. Westbrook, Z. Feng, G. Gilliland, T.N. Bhat, H. Weissig, I.N. Shindyalov, P.E. Bourne, Nucleic acids research, 28 (2000) 235-242.
[34] T. Bertrand, N.A. Eady, J.N. Jones, Jesmin, J.M. Nagy, B. Jamart-Gregoire, E.L. Raven, K.A. Brown, The Journal of biological chemistry, 279 (2004) 38991-38999.
[35] P. Lempens, C.J. Meehan, K. Vandelannoote, K. Fissette, P. de Rijk, A. Van Deun, L. Rigouts, B.C. de Jong, Scientific reports, 8 (2018) 3246.
[36] N. Guex, M.C. Peitsch, Electrophoresis, 18 (1997) 2714-2723.
[37] G.M. Sastry, M. Adzhigirey, T. Day, R. Annabhimoju, W. Sherman, J Comput Aided Mol Des, 27 (2013) 221-234.
[38] G.M. Morris, R. Huey, W. Lindstrom, M.F. Sanner, R.K. Belew, D.S. Goodsell, A.J. Olson, J Comput Chem, 30 (2009) 2785-2791.
[39] V. Zoete, M.A. Cuendet, A. Grosdidier, O. Michielin, J Comput Chem, 32 (2011) 2359-2368.
[40] R. Kumari, R. Kumar, A. Lynn, Journal of Chemical Information and Modeling, 54 (2014) 1951-1962.
[41] M.A. Islam, T.S. Pillay, Journal of biomolecular structure & dynamics, 37 (2019) 503-522.
[42] C.A. Lipinski, F. Lombardo, B.W. Dominy, P.J. Feeney, Adv Drug Deliv Rev, 46 (2001) 3-26.
[43] D.F. Veber, S.R. Johnson, H.Y. Cheng, B.R. Smith, K.W. Ward, K.D. Kopple, J Med Chem, 45 (2002) 2615-2623.
[44] Y. Fukunishi, T. Kurosawa, Y. Mikami, H. Nakamura, J Chem Inf Model, 54 (2014) 3259-3267.
[45] G. Srivastava, S. Tripathi, A. Kumar, A. Sharma, Tuberculosis, 105 (2017) 18-27.
[46] G.S. Timmins, V. Deretic, Mol Microbiol, 62 (2006) 1220-1227.
[47] M.J. Jedrzejas, S. Singh, W.J. Brouillette, G.M. Air, M. Luo, Proteins, 23 (1995) 264-277.
[48] J.P. Hughes, S. Rees, S.B. Kalindjian, K.L. Philpott, Br J Pharmacol, 162 (2011) 1239-1249.
[49] C.H. Reynolds, R.C. Reynolds, J Chem Inf Model, 57 (2017) 3086-3093.
[50] A.L. Hopkins, C.R. Groom, A. Alex, Drug Discov Today, 9 (2004) 430-431.
[51] C.H. Reynolds, S.D. Bembenek, B.A. Tounge, Bioorg Med Chem Lett, 17 (2007) 4258-4261.
[52] S. Schultes, C. de Graaf, E.E.J. Haaksma, I.J.P. de Esch, R. Leurs, O. Kra¨mer, Drug Discov Today Technol, 7 (2010) e147-202.
[53] G.M. Keseru, G.M. Makara, Nat Rev Drug Discov, 8 (2009) 203-212.
[54] K.O. Sulaiman, T.U. Kolapo, A.T. Onawole, A. Islam, R.O. Adegoke, S.O. Badmus, Journal of biomolecular structure & dynamics, (2018) 1-31.